Hollow Fiber Membranes Spun from Lewis Acid : Base Complexes. I. Structure Determination by Oxygen Plasma Ablation

A. K. FRITZSCHE, *Romicon, Woburn, Massachusetts 01801,*
C. A. CRUSE, R. E. KESTING, and M. K. MURPHY*, *Permea Inc., A Monsanto Company, St. Louis, Missouri 63146*

Synopsis

The structures of polysulfone hollow fiber membranes, spun from the propionic acid : *N*-methylpyrrolidone complex and from a formylpiperidine/formamide mixture were investigated as a function of progressive surface removal with an oxygen plasma. Oxygen plasma ablation experiments were performed on both unexposed and isopentane-treated hollow fiber membranes. Pure gas permeation rates were obtained on these samples as well as oxygen plasma etched samples which were then subsequently coated with polydimethyl–siloxane from an isopentane solution. The results show that the hollow fiber membrane spun from the propionic acid : *N*-methylpyrrolidone complex has both a thinner active separating layer and a thinner skin than the polysulfone hollow fiber membrane spun from the formylpiperidine/formamide mixture. Also, the resistance to flow of the porous substrate of the complex spun hollow fiber membrane is significantly less than that of the polysulfone hollow fiber membrane spun from the mixture. Therefore, the substrate of the PA : NMP complex spun hollow fiber membrane has greater porosity and less tortuosity than its FP/FA congener. The oxygen plasma ablation results and the scanning electron micrographs demonstrate a nonequivalence between the active separating layer and the microscopically observable skin of the hollow fiber membrane. It is believed that membranes prepared from Lewis acid : base complex solvents possess a porous substructure and a nonuniform (graded-density) skin which consists of a very thin active separating layer whose effective thickness varies depending upon the gases to be separated and a thin less dense transition layer, which may contain pores whose sizes are below the limits of resolution by SEM. Both are components of the microscopically observable skin. Membranes possessing this structure belong to the trilayer class of integrally skinned membranes. If membranes are so fabricated that the density gradient in the active separating layer approaches zero, a bilayer membrane with a porous substructure and a thin skin of uniform density results. Membranes prepared from conventional solvent/nonsolvent mixtures, i.e., formylpiperidine/formamide, exhibit a diminished density gradient in the skin approximating the bilayer model.

INTRODUCTION

In 1960 Loeb and Sourirajan invented the first integrally skinned membrane for desalination by phase inversion of cellulose acetate sols.[1] In the integrally skinned membrane, the skin and substructure are composed of the same material. The skin layer determines both the permeability and selectivity of the bilayer, whereas the porous substructure functions primarily as a physical support for the skin. Differences in density between the two layers are the result of interfacial forces and the fact that solvent loss occurs more rapidly

*Author to whom inquiries should be addressed.

Journal of Applied Polymer Science, Vol. 40, 19–40 (1990)

CCC 0021-8995/90/1-20019-22$04.00

from the air–solution and solution–coagulation bath interfaces than from the solution interior.[2]

Integrally skinned hollow fiber membranes suitable for commercial gas separations were subsequently developed by application of a special coating procedure.[3] A thin layer of a highly permeable, nonselective polymer was applied to the surface of an asymmetric polysulfone hollow fiber membrane. This coating sufficiently reduces the permeability through the pores and defects within the skin to render permeation through the normal skin layer predominant. As in the cellulose acetate membrane, the internal matrix of the hollow fiber does not affect gas separation, but it does offer resistance to passage of gases through the hollow fiber.

Exposure of these integrally skinned hollow fiber membranes to an oxygen plasma has proven itself a viable procedure for investigating the hollow fiber membrane structure. With electrodeless radio-frequency excitation, diatomic oxygen molecules are disassociated into free radicals and ions. At low pressures, these moieties are sufficiently long-lived to react with a variety of polymers, which is reflected by a loss of weight with time.[4,5] The rate of ablation is dependent upon the chemical structure of the polymer as well as the radio-frequency power level and the oxygen flow rate.[4-6] The plasma treatment has been found to be confined to the surface regions of a polymer and does not alter its bulk properties.[7-11] For this reason, plasma treatment has been used to alter polymer adhesive bondability and wettability[6,11-17] as well as to study surface morphology.[8,18-22] An additional advantage is that oxygen plasma ablation is a low temperature process.[4] Therefore, the internal structure of the sample remains unaltered by thermal effects.

Oxygen plasma ablation has been used successfully to define the structure of polysulfone hollow fiber membranes.[23] In this paper, the results of oxygen plasma ablation studies to define the structures of polysulfone hollow fiber membranes spun from propionic acid : *N*-methylpyrrolidone Lewis acid : base complexes and from formylpiperidine/formamide mixtures will be presented.[24]

EXPERIMENTAL

Test cells were prepared from hollow fiber membranes spun from 37% total solids polysulfone (Amoco Udel P3500) dopes in 43 wt % propionic acid: 57 wt % *N*-methylpyrrolidone Lewis acid : base complex and 87 wt % formyl piperidine/13 wt % formamide solvent/nonsolvent mixture. The same lot of polysulfone was used to prepare all the hollow fiber membranes in this investigation. In this discussion, a slash between the solvent and nonsolvent indicates that the pair is noncomplexed. A colon indicates complex formation. Each test cell contained 18 hollow fibers approximately 15 cm in length. One end of the collection was encapsulated in a 3/8 in. diameter seal. This seal fixes the cell in the gas tester and prohibits intermixing of the feed and product gases. The other end of the hollow fiber membrane array was closed with a drop of rapid curing epoxy. Therefore, the only gas flow measured during testing is that which is transported across the hollow fiber membranes. Twenty-six test cells of each type were made. These test cells were divided into two sets. The first set contained 16 test cells of each type of hollow fiber membrane. Duplicate samples of each type were placed in a Tracerlab low

temperature asher for exposure to an oxygen plasma for 0.5, 1.0, 1.5, 2.0, 3.0, 5.0, or 10.0 min. Duplicate samples of each type remained unexposed controls. The oxygen plasma was maintained with a radio frequency of 13.6 MHz at a power level of 50 W. The oxygen flow rate was 20 sccm.

These samples were measured for their uncoated helium and nitrogen permeabilities at 100 psig at room temperature. The hollow fiber membranes were then coated from a 0.5% Sylgard solution and retested for helium and nitrogen flux rates at 600 psig at room temperature. During the coating procedure not only does Sylgard plug the pores and defects in the separating layer,[3] but the isopentane solvent alters the hollow fiber membrane morphology. In order to separate the effects of coating and isopentane solvent, the second set of test cells was subjected to the coating procedure without the Sylgard coating present. Duplicate samples of each type of hollow fiber membrane were then oxygen plasma ablated under the same conditions for 1.0, 2.0, 3.0, and 5.0 min. Again, duplicate samples of each were maintained as unexposed controls. The helium and nitrogen flux rates of these samples were also obtained at 100 psig at room temperature. The helium and nitrogen permeabilities were calculated by

$$\frac{P}{l} = \frac{Q}{A\,\Delta P} = \frac{Q}{n\pi DL\,\Delta P} \tag{1}$$

where P = the permeability of the separating layer cm^3(STP)-cm/cm^2-sec-cm Hg, l = the effective thickness of the separating layer (cm), Q = the gas flux, n = number of fibers in the sampling, D = outer diameter of the hollow fiber membrane, L = active length of the fibers, and ΔP = differential pressure between outer surface and bore of the hollow fiber membrane.

The separation factor, also referred to as the selectivity, of the gas pair is ratio of their permeation rates. For a gas pair, such as helium and nitrogen, the separation factor is given by

$$\alpha = \frac{P/l(\mathrm{He})}{P/l(\mathrm{N_2})} \tag{2}$$

The ablation rate of oxygen plasma of polysulfone was determined by measuring the loss of weight per unit time on melt pressed films of known surface area. The ablation rate can be calculated by

$$A = \frac{\Delta W}{\rho S \Delta t} \tag{3}$$

where A = the ablation rate (cm/min), ΔW = change in weight (g), ρ = density of polysulfone (1.24 g/cm^3), S = the surface area of the film (cm^2), and Δt = the time period in which the measured weight change occurred (min). The oxygen plasma ablation rate under the conditions of this series of experiments was calculated to be 11.2 $\pm$ 1 nm/min. This ablation rate, determined from melt pressed films, can be used to estimate the effective separating layer thickness of an integrally skinned hollow fiber membrane if two

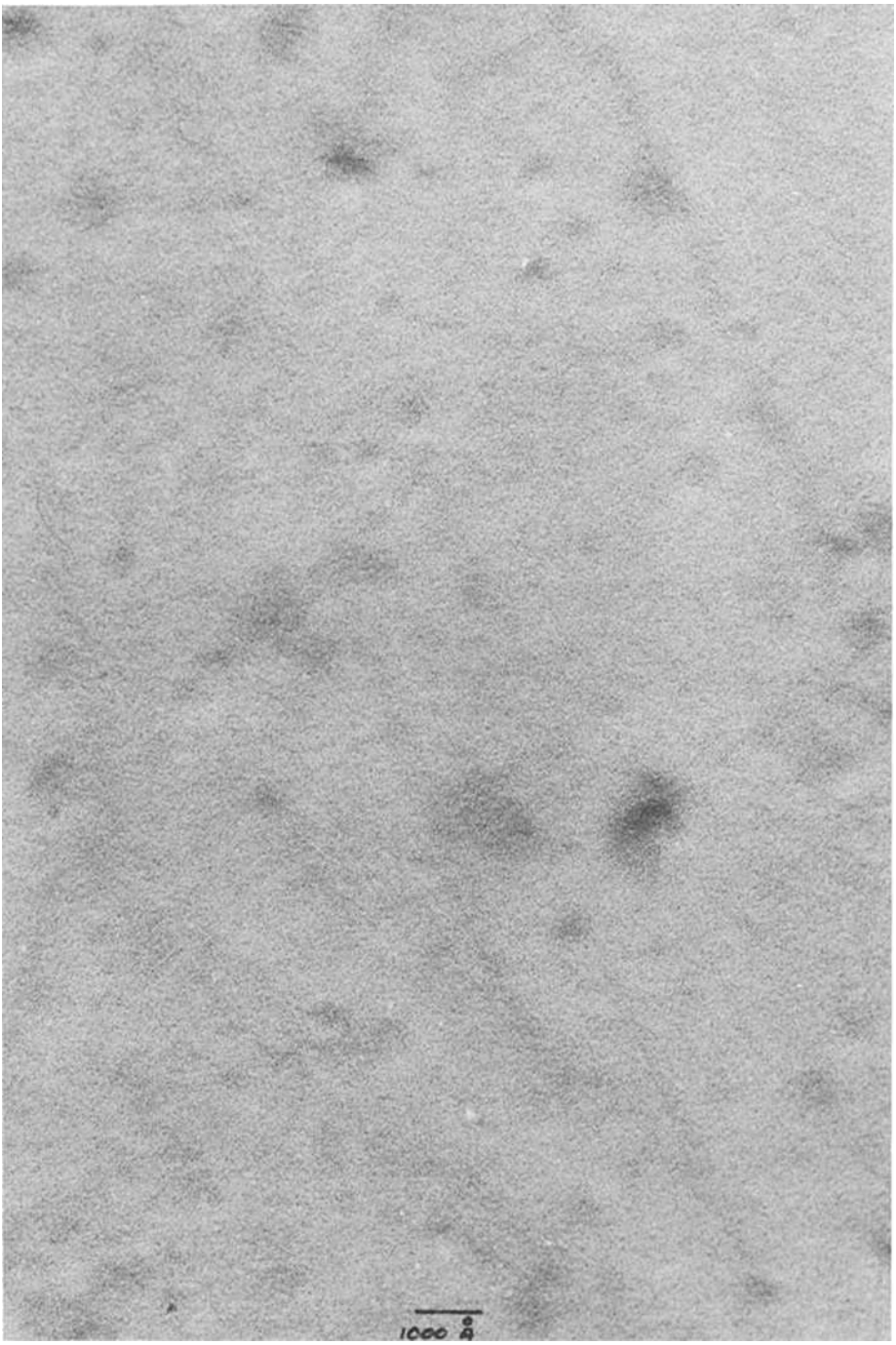

Fig. 1. Transmission electron micrograph of a surface replica of a melt-pressed polysulfone film.

Fig. 2. Transmission electron micrograph of a surface replica of a polysulfone hollow fiber membrane.

assumptions are made. First, the oxygen plasma ablation rate is independent of free volume differences among melt pressed films arising from differences in their thermal history and among the skins of hollow fiber membranes arising from variations in their spinning conditions, coagulation rates, and speed and completeness of solvent removal. Second, the surfaces of both the melt pressed films and the hollow fiber membranes have the same degree of smoothness.

The validity of the first assumption is supported by the loss of weight of skins of hollow fiber membranes as a function of oxygen plasma exposure time. The initial oxygen plasma ablation rates of hollow fiber membranes spun from the Lewis acid : base complex and the noncomplexing solvent system are equivalent within experimental $1.4 \pm 0.2 \times 10^{-6}$ g/min cm^2 and are equivalent to those obtained with melt pressed polysulfone films. After this initial slow removal rate, the etching rate increases rapidly. This increase in ablation rate approximately coincides with the points on the permeability curves where the curvature changes to linear and is attributed to penetration of the oxygen plasma into the porous substructure. It is also supported by the oxygen plasma etching studies of Lawton on amorphous and semicrystalline films of poly(ethylene terephthalate) (PET) and isotactic polystyrene (PS).[25] His results showed that the rates of weight loss are independent of the degree of crystallinity at any given discharge power at constant oxygen flow rate for both PET and PS. The polymer chains in the crystalline regions are more highly ordered and the crystalline density is much greater than an amorphous glass.

Yet, polymeric material is removed from each zone with equal rapidity. If ablation rate were free volume dependent, the amorphous PS and PET samples would exhibit higher ablation rates than the semicrystalline materials, and the ablation rates would decrease with increasing percent crystallinity. The same paper includes oxygen ablation measurements on a biaxially oriented film of PET. According to Ringwald,[26] the T_g of PET increases from 81 to 125°C upon orientation, implying a substantial increase in free volume in the amorphous regions upon orientation. Yet, the ablation rate remains the same.

The second assumption is needed because a rough, irregular surface has a greater surface area than a smooth, uniform surface, even though both are enclosed by the same boundaries. Therefore, a film with a rough surface would exhibit a greater weight loss per unit time than the smoother because more polymer chains would be accessible to ablation by the oxygen plasma. Transmission electron micrographs of surface replicas of melt pressed films (Fig. 1) and solution spun polysulfone hollow fiber membranes (Fig. 2) indicate that the solution spun fiber does have some major surface irregularities in comparison to the melt pressed film, but the fine structures of the two are similar. Therefore, one would predict that the assumption is valid within the limits of experimental error.

RESULTS AND DISCUSSION

The helium and nitrogen permeabilities of untreated, i.e., neither Sylgard-coated nor isopentane-exposed, polysulfone hollow fiber membranes spun from both the formylpiperidine/formamide (FP/FA) and propionic acid : *N*-meth-

TABLE I
Performance of Uncoated, Unexposed Polysulfone Hollow Fiber Membranes as Function of Oxygen Plasma Exposure Time

Etch time (min)	Formylpiperidine/formamide			Propionic Acid : NMP		
	$P/l(He)^a \times 10^6$	$P/l(N_2)^a \times 10^6$	α	$P/l(He)^a \times 10^6$	$P/l(N_2)^a \times 10^6$	α
0	49.4	5.98	11.6	478	139	3.4
0	56.3	3.46	16.3	482	144	3.4
0.5	48.0	4.05	11.9	873	331	2.6
0.5	47.8	2.11	28.7	801	282	2.9
1.0	49.0	5.66	8.7	810	316	2.6
1.0	65.2	6.19	10.5	651	245	2.7
1.5	88.1	19.1	4.6	1672	732	2.3
1.5	103.7	24.7	4.2	1458	609	2.4
2.0	110.9	30.2	3.7	1545	675	2.3
2.0	174	56.3	3.1	2118	1011	2.1
3.0	159	52.2	3.1	2876	1413	2.0
3.0	187	65.9	2.8	2662	1305	2.0
5.0	203	71.4	2.9	2565	1243	2.1
10.0	174	124	1.4	2894	1453	2.0
10.0				2876	1422	2.0

[a]All permeability units are $cm^3(STP)/cm^2$ s cm Hg.

ylpyrrolidone dopes as a function of oxygen plasma exposure time are given in Table I.

The results for uncoated fiber which were exposed to isopentane prior to oxygen plasma exposure are given in Table II, and Table III gives the helium and nitrogen permeation rates and separation factors of etched samples which were subsequently coated from a 0.5% Sylgard solution. The results in these tables are illustrated graphically in Figures 3–7, where Figures 3 and 4 compare the helium/nitrogen permeabilities and separation factors of the

TABLE II
Performance of Uncoated, Isopentane Exposed Polysulfone Hollow Fiber Membranes as Function of Oxygen Plasma Exposure Time

Etch time (min)	Formylpiperidine/formamide			Propionic Acid : NMP		
	$P/l(He)^a \times 10^6$	$P/l(N_2)^a \times 10^6$	α	$P/l(He)^a \times 10^6$	$P/l(N_2)^a \times 10^6$	α
0	64.4	1.12	57.5	193	10.3	18.7
0	57.4	0.81	70.9	173	8.5	20.3
1	60.5	10.8	5.6	1298	556	2.4
1	135.4	40.3	3.4	1184	492	2.4
2	237	87.0	2.7	2507	1206	2.0
2	204	71.6	2.9	2196	1048	2.1
3	197	69.0	2.9	2211	1078	2.1
3	145	47.3	3.1	2360	1171	2.0
5	347	139	2.5	2710	1357	2.0
5	312	121	2.6			

[a]All permeabilities in units of $cm^3(STP)/cm^2$ s cm Hg.

TABLE III
Performance of Sylgard Coated Polysulfone Hollow Fiber Membranes as Function of Oxygen Plasma Exposure Time

Etch time[a] (min)	Formylpiperidine/formamide			Propionic Acid : NMP		
	P/l(He)[b] $\times 10^6$	$P/l(N_2)$ $\times 10^6$	α	P/l(He) $\times 10^6$	$P/l(N_2)$ $\times 10^6$	α
0	58.1	0.52	111	191	2.27	84.1
0.5	41.8	0.36	116	100	2.26	44.3
1.0	46.6	0.36	131	121	1.68	72.3
1.5	46.2	0.51	91	150	5.42	27.7
2.0	48.7	0.58	84	126	6.04	20.9
3.0	45.0	0.66	68	123	78	1.58
5.0	50.2	1.22	41.2	139	85	1.63
10.0	67	10.0	6.7	134	141	0.95

[a]Samples coated after oxygen plasma exposure.
[b]Permeability units in $cm^3(STP)/cm^2$ s cm Hg.

PA : NMP untreated hollow fiber membranes with those obtained from the formylpiperidine/formamide as a function of oxygen plasma exposure time. In Figures 5 and 6, the effects can be compared of the isopentane treatment and the Sylgard coating on the helium and nitrogen permeabilities as a function of oxygen etch time on the hollow fiber membranes spun from formylpiperidine/formamide and propionic acid : *N*-methylpyrrolidone, respectively. The changes in helium/nitrogen separation factors vs. oxygen etch time for hollow fiber membranes spun from both FP/FA and PA : NMP which were either untreated, isopentane-treated, or coated from a 0.5%Sylgard solution are shown in Figure 7. The helium and nitrogen permeation results, given in Table I and shown in Figure 3, for the uncoated and unexposed hollow fiber membranes reveal major differences between the structures of the two hollow fiber membranes. The helium permeability of the unetched hollow fiber membranes spun from PA : NMP is about seven times greater than its unetched FP/FA congener. Its nitrogen permeability is at least 20 times greater. Sequential removal of the outer layers of the hollow fiber membranes results in slight changes in both the helium and nitrogen permeabilities in the first minute of oxygen plasma ablation followed by a rapid rise in these values during the second minute of etching with a gradual rise thereafter for the FP/FA hollow fiber membrane as shown in Figure 3. In contrast, the etched hollow fiber membranes from PA : NMP dopes exhibit only increases in both helium and nitrogen flux with ablation throughout the first 2 min of etching followed by a slower rate of increase in flux rates as additional surface is removed. The high transport rates of the PA : NMP spun hollow fiber membrane in contrast to those of the FP/FA spun hollow fiber membranes after the separating layer has been removed, i.e., after 2 min oxygen plasma exposure, show that the separating layer substructures of these two hollow fiber membranes are significantly different. The PA : NMP hollow fiber membranes possess greater porosities in their substructures than the FP/FA hollow fiber membranes.

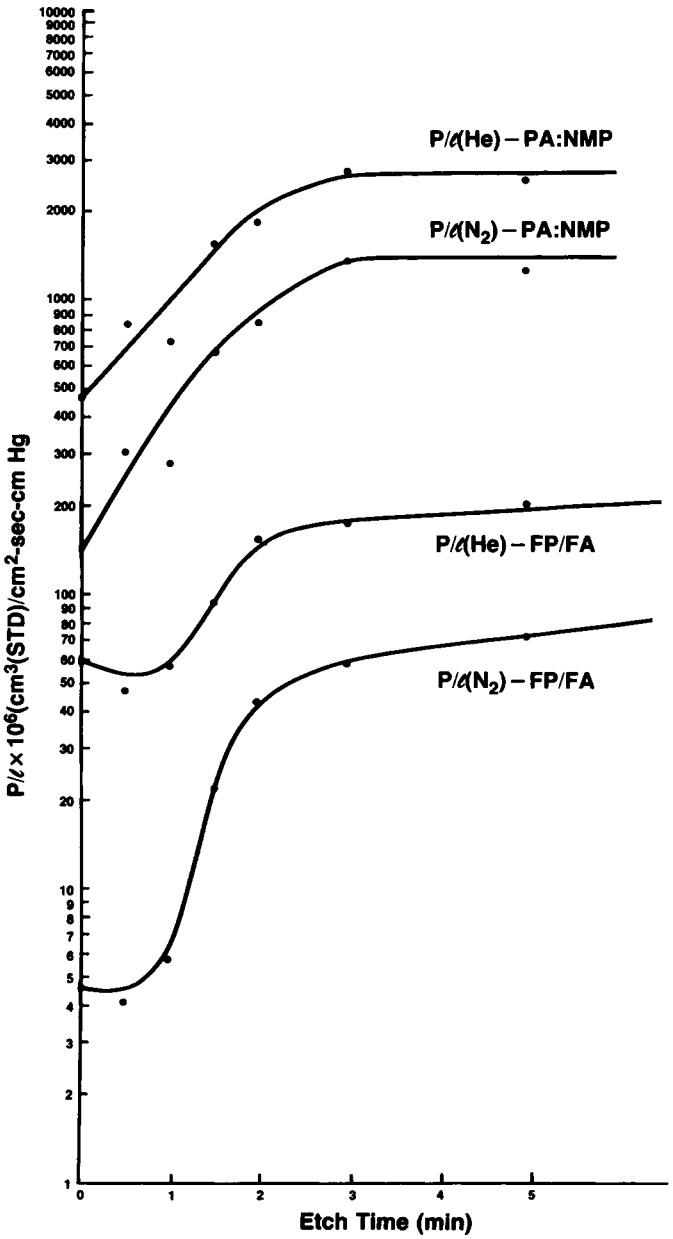

Fig. 3. Helium and nitrogen permeabilities of untreated polysulfone hollow fiber membranes spun from PA : NMP complexes and FP/FA mixtures as function of oxygen plasma exposure time.

The separation factors measured as a function of oxygen plasma ablation time, given in Table I, are shown in Figure 4 for uncoated, untreated hollow fiber membranes spun from FP/FA mixtures and PA : NMP. Dramatic differences between the two can be seen. The hollow fiber membranes spun from FP/FA has a much higher initial separation factor, at least three times that

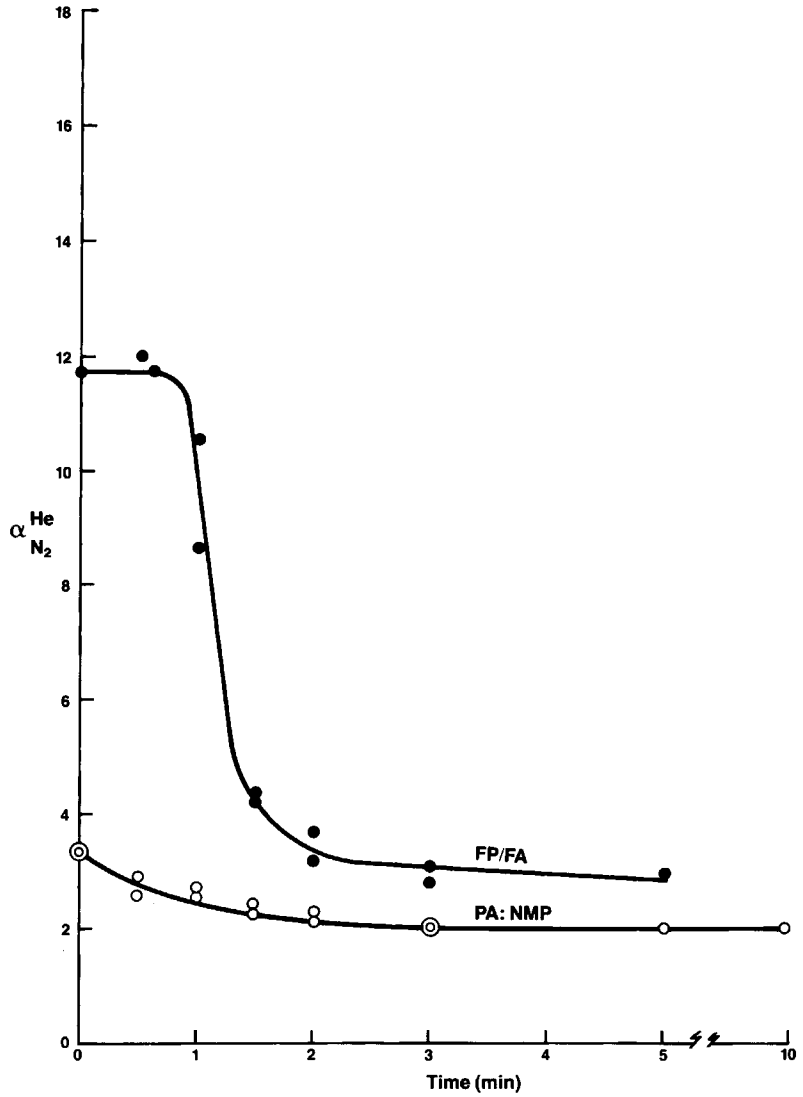

Fig. 4. Comparison of changes in the separation factor with oxygen plasma exposure time of polysulfone hollow fiber membranes spun from PA : NMP and from FP/FA.

obtained with the PA : NMP spun hollow fiber membrane. Because separation factor is independent of separating layer thickness, the higher separation factor from the FP/FA spun hollow fiber membrane indicates that its effective separating layer is tighter with fewer pores and defects than the effective separating layer of the PA : NMP spun hollow fiber membrane. The separation factor of the FP/FA spun hollow fiber membrane shows little change during the first 30–60 s of etching. Then an abrupt decline in separation factor occurs during the subsequent 30–90 s followed by a slow, gradual drop in separation factor with additional plasma ablation. These results imply a dense effective separating layer around 6–12 nm thick. Beneath this effective separating layer is a transitional zone, approximately 12–18 nm thick, which

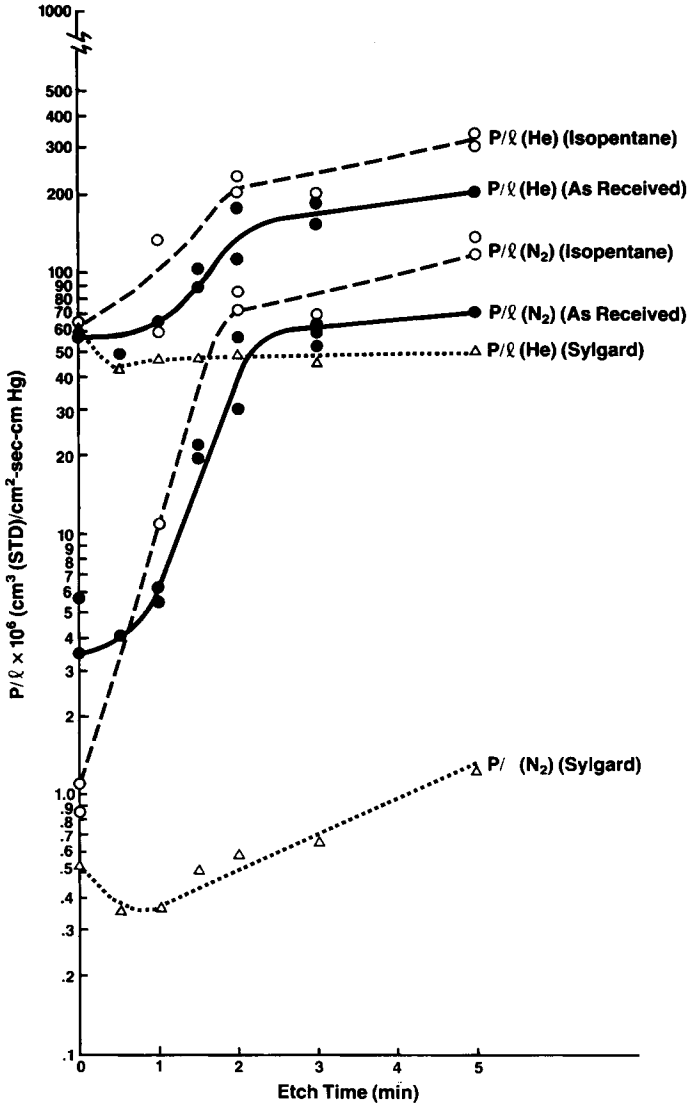

Fig. 5. Variation in helium and nitrogen permeability of polysulfone hollow fiber membranes spun from FP/FA as function of oxygen plasma exposure time.

may contain micropores. In this zone, the structure of the layer changes from one similar to the separating layer to one similar to the internal porous matrix. In the hollow fiber membranes spun from PA : NMP, no plateau is observed within the limits of detection of the experiment, and the change in separation factor is gradual as one traverses from the outer surface of the membrane to the supporting matrix. If the separating layer were defined as the time required for the change in separation factor to become linear with time, i.e., at 2 min oxygen plasma ablation in Figure 4, then the separating layer (effective separating layer plus the transitional zone) of both membranes appear to be the same. Yet, it is the effective separating layer of the hollow fiber membrane, i.e., the outer surface layer, which controls the membrane

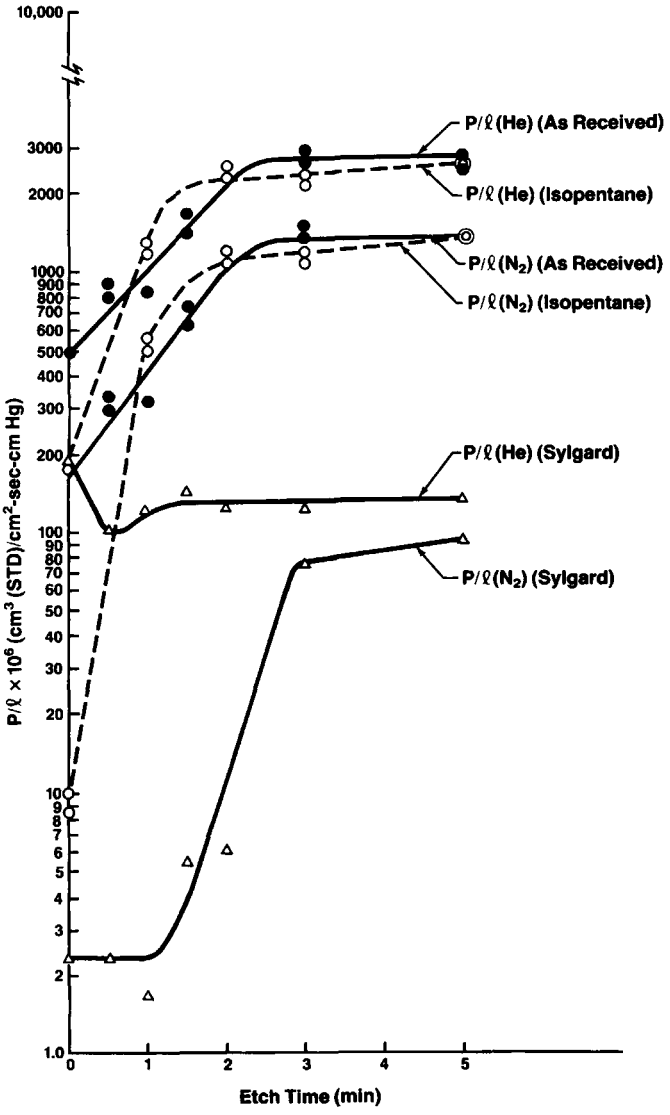

Fig. 6. Variation in helium and nitrogen permeability of polysulfone hollow fiber membranes spun from PA : NMP complexes as function of oxygen plasma exposure time.

performance. Polysulfone hollow fiber membranes are not usually used uncoated for gas separations, but they are coated with Sylgard, a polydimethylsiloxane, from isopentane solution. The coating serves to plug the pores and defects in the hollow fiber membrane surface to force the permeating moiety through the separating layer of the hollow fiber membrane.

The influence of this process on hollow fiber membranes spun from both FP/FA and PA : NMP was also explored. Table II gives the performance of uncoated polysulfone hollow fiber membranes which had been exposed to isopentane prior to oxygen plasma ablation. Table III lists the results for hollow fiber membranes which had been coated with Sylgard after oxygen

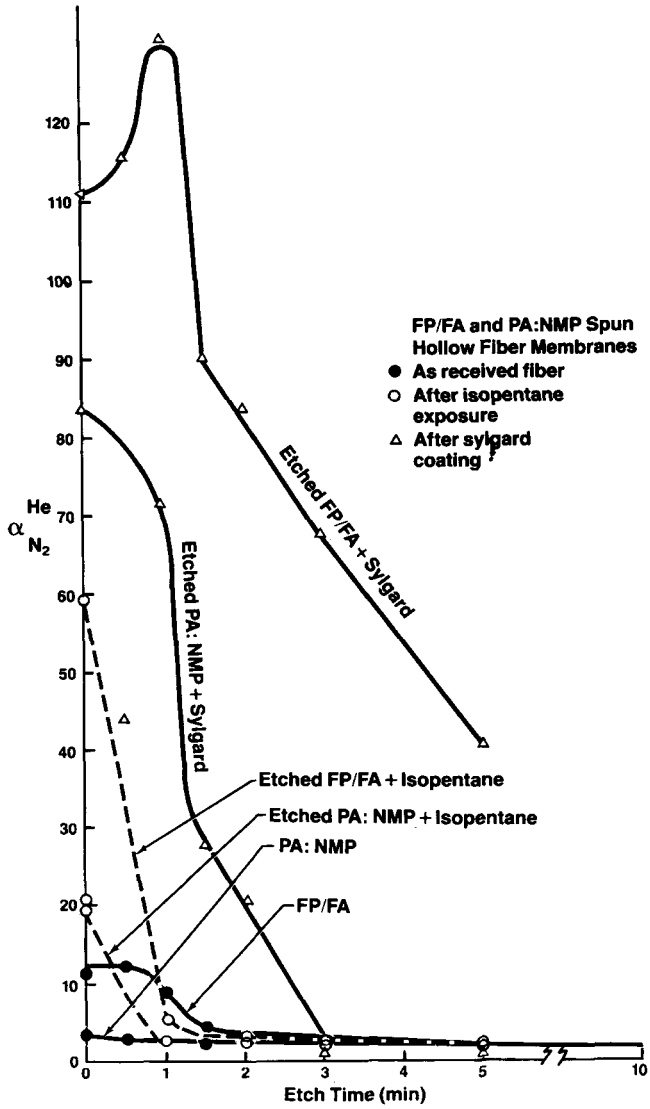

Fig. 7. Change in the separation factor of helium and nitrogen of polysulfone hollow fiber membranes spun from FP/FA mixtures and PA : NMP complexes as function of oxygen plasma exposure time.

plasma ablation. The results are also illustrated graphically in Figures 5–7 for the gas transport of FP/FA membranes, for gas transport of PA : NMP membranes, and for the change in separation factor with each treatment, respectively. The effect of isopentane exposure on the hollow fiber membranes is dramatic. The nitrogen permeability of the FP/FA spun hollow fiber membrane dropped from 5.98 to 1.12×10^{-6} upon exposure to isopentane, yielding a fivefold increase in separation factor. Similarly, the nitrogen permeability of the PA : NMP spun hollow fiber membrane declined from 139 to 10.3×10^{-6} with isopentane treatment. A fivefold increase in separation

factor was also seen. The decrease in gas transport rates and increase in separation factors resulted from closure of small pore and defects in the surface of the hollow fiber membrane by interaction with isopentane. With surface porosity reduced, a larger fraction of the gases were transported through the membrane material in the effective separating layer than through the pores. Consequently, flux declined as flow through the pores was reduced and separation factor increased. The isopentane treatment also altered the glass transition temperatures of the hollow fiber membrane. The glass transition temperature, determined by the first heat from a DSC scan of the unexposed FP/FA spun fiber, containing 1.45% residual FP, is 171°C.[27] The T_g increase to 178°C is attributed to lowering the residual formylpiperidine content by its extraction with isopentane. The decline in the glass transition temperature in the PA : NMP spun hollow fiber membranes from 195° to 193°C is attributed to a decline in free volume induced by isopentane.

The isopentane treatment also appears to alter the internal structure of the hollow fiber membranes as well as the structure of the outer separating layer. While flux declined and separation factor increased at the outer layer of the membranes with isopentane exposure, the opposite occurred in the interior of the hollow fiber membrane. When the performance of an isopentane exposed hollow fiber membrane is compared with that of the identical membrane not exposed to isopentane and etched for identical periods of time, the former also exhibits higher flux rates and lower separation factors. It appears that, although isopentane densifies the polymeric material in the separating layer, it simultaneously decreases resistance to transport in the interior.

Comparison of the helium and nitrogen permeation rates for isopentane treated fiber in Figure 5 for FP/FA spun membrane and Figure 6 for the PA : NMP spun membrane reveal that each plot consists of two straight lines. The first is one of rapidly increasing flux rate with oxygen exposure time and the second is one with a gradual increase in flux with additional oxygen plasma ablation. If the point intersection of these two lines were defined as the time needed to remove the effective separating layer in an isopentane treated hollow fiber membrane, then the effective separating layer thickness can be determined, which is about 22.4 $\pm$ 1 nm for the FP/FA spun hollow fiber membrane and about half that for the PA : NMP spun hollow fiber membrane. Because isopentane is used as the carrier solvent for the Sylgard coating, the coated hollow fiber membranes would have effective separating layers equivalent in thickness to the isopentane treated membranes. Therefore, the results suggest that the effective separating layer thickness, free volume, and density gradient can be influenced not only by spinning solvent composition, dope total solids level, and spinning conditions but by the nature of the coating carrier solvent.

Examination of the Sylgard coated hollow fiber membrane results in Table III and Figures 5–7 reveals that the unetched hollow fiber membranes follow the Henis–Tripodi resistance model.[28] The pores and defects are filled with polydimethylsiloxane coating, thus dramatically reducing their capacity to transport gas. Consequently, permeation is restricted to the polysulfone in the separating layer. Coating primarily affects the slow gas. A much larger percentage of the total gas transport of the slow gas is through the pores and defects of the separating layer than for the fast gas. Therefore, coating

dramatically reduces slow gas flux in contrast to the fast gas with a concomitant increase in separation factor. As the outer layers of the membrane are removed by the oxygen plasma, the interior of the hollow fiber membrane beneath the effective separating layer is exposed. As one proceeds into the hollow fiber membrane both the porosity and the average pore size increases. A larger and larger fraction of the surface of the coated hollow fiber membrane consists of pores plugged with silicone rubber. As the membrane becomes more like a composite membrane, i.e., a porous matrix coated with a silicone rubber, the separation factor drops. In the PA : NMP spun hollow fiber membrane, the separation factor drops to 1.58 after 3 min of etching. This helium/nitrogen separation factor is that which is expected from a silicone rubber film.[29,30] After 10 minutes of oxygen plasma ablation, pores of such size as not to be effectively plugged by the coating are reached, and no separation of the gases can be effected. One would suspect that, as the exposed pores become sufficiently large, the silicone coating would be carried into and be deposited on the porous substructure. Initially, such deposition would have little impact on permeability due to the open structure of the matrix. However, significant deposition would create obstructions to gas transport to reduce the gas flux across the membrane. Examination of the results in Table III implies that the PA : NMP hollow fiber membrane has a structure composed of a dense, effective separating layer about 11.2 ± 1.1 nm thick, a transitional zone of equivalent thickness of increasing porosity, and average pore size in which the pores are sufficiently small to be effectively coated, and a highly porous matrix in which the pores are beyond the size to be effectively plugged by the coating.

The hollow fiber membrane spun from FP/FA possessed a denser active separating layer approximately twice as thick as the one observed for the hollow fiber membrane spun from PA : NMP. The gradient in porosity increase and pore size increase is also smaller for the FP/FA spun hollow fiber membrane than its congener. After 10 min of oxygen ablation, the separation factor did not drop to that expected from a silicone rubber film. This indicates that the transitional zone is at least 90.0 ± 9.0 nm thick for these hollow fiber membranes.

Hollow fiber membranes prepared from the PA : NMP complex and the FP/FA mixture were submitted for SEM analysis. The JEOL JSM-840 scanning electron microscope was used to study the untreated, unetched hollow fiber membranes. The outer edges of the two hollow fiber membranes are shown in Figures 8 and 9. The morphological differences between the two are quite striking. The SEM photomicrograph of the outer edge of the PA : NMP complex spun hollow fiber membrane reveals a gradual transition from the outer surface to the supporting matrix. The presence of a skin is evident, but it is difficult to determine the inner boundary. It appears that the skin is 300–500 nm thick and that the skin becomes more dense as one proceeds from the membrane interior towards the outer surface. One observes pores and channels which diminish in size until their dimensions are below the limit of resolution of the SEM, which is 4 nm at best. The oxygen plasma ablation studies suggest an active separating layer of 10–12 nm for this hollow fiber membrane, which is only a small fraction of the observable skin defined by SEM. From these photomicrographs and the plasma results, one must

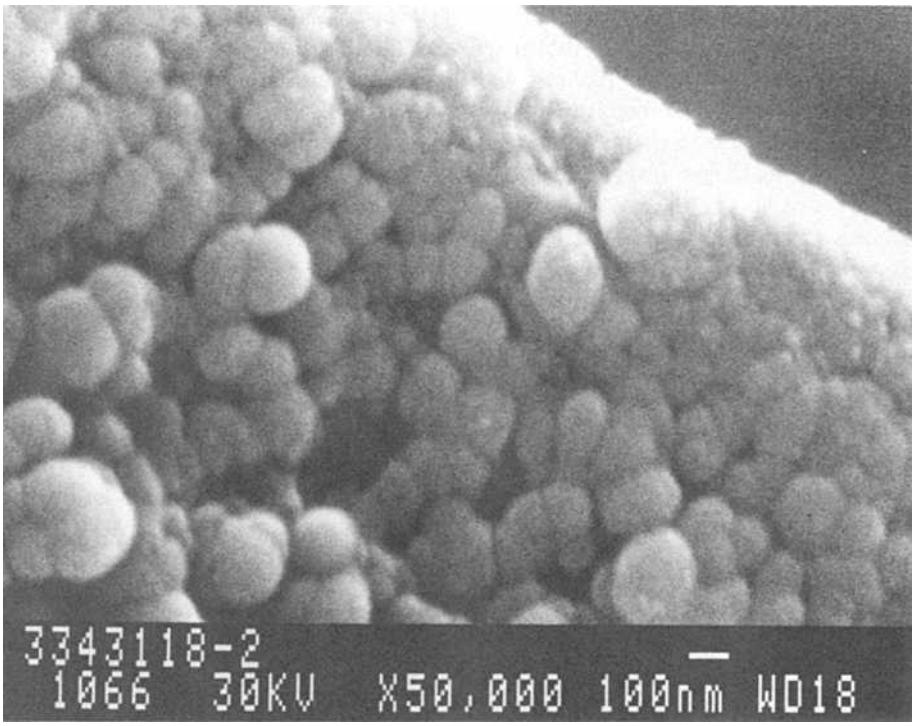

Fig. 8. Scanning electron micrograph of the outer edge of an unetched, untreated hollow fiber membrane spun from PA : NMP complex.

conclude that the active separating layer and the skin are nonequivalent and that the former is only a small fraction of the latter.

The photomicrograph of the hollow fiber membrane spun from the FP/FA mixture (Fig. 9) reveals a distinct boundary between the skin and the supporting matrix. The skin appears denser and more uniform than the skin of the membrane spun from the PA : NMP complex as well as thicker, that is, about 600 nm. Since the oxygen plasma results suggest that the active separating layer is 20–24 nm thick, the effective separating layer is also only a fraction of the microscopically observed skin. One then must conclude that both hollow fiber membranes have a density gradient across their microscopically observable skins, but the density gradient in the complex spun hollow fiber membrane is greater than that of its FP/FA spun cogener. The existence of a difference in the density gradients in the active separating layers which progresses also through the microscopically observable skins implied to the authors that this density gradient can be manipulated to yield a new class of integrally skinned gas separation membranes, designated as trilayer membranes. A trilayer membrane possesses a porous substructure and a nonuniform (graded density) skin. This skin consists of a very thin dense active separating layer, whose effective thickness varies depending upon the gases to be separated, and an underlying less dense transition layer. Both are components of the microscopically observable skin. The determination of the thickness of this skin is limited by the resolution of microscope. The trilayer

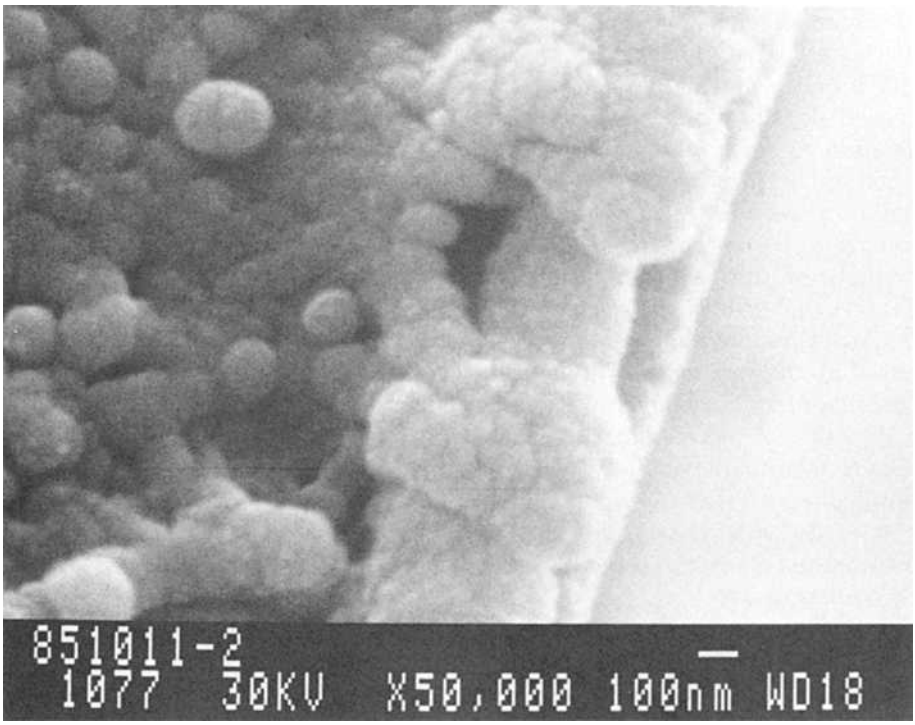

Fig. 9. Scanning electron micrograph of the outer edge of an unetched, untreated hollow fiber membrane spun from FP/FA mixture.

structure is attained by controlling the kinetics of gelation and desolvation through the use of a solvent system containing a Lewis acid and a Lewis base to yield 1 : 1 Lewis acid : base complex. The Lewis acid is an electron pair acceptor and the Lewis base an electron pair donor. Together they form the complex

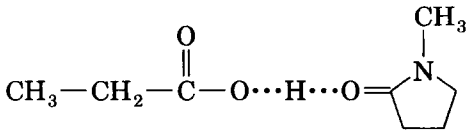

which dissociates into its components upon contact with water. Formation of the complex permits sequestering of much larger amounts of nonsolvent into the spinning dope with maintenance of dope stability than can be achieved with classical solvent/nonsolvent mixtures. Exposure to water during coagulation disrupts the complex accelerating the sol-to-gel transition. The dissociation of the complex into its smaller constituents facilitates rapid and complete solvent removal during coagulation, fixing its structure by limiting the time available for conformational rearrangements. The resultant membrane possesses increased free volume as evidenced by an elevated glass transition temperature observed on the initial thermal excursion in differential scanning calorimetry. These measured glass transition temperatures are higher than both those of the polymer from which the membrane is fabricated and those

of asymmetric hollow fiber membranes, which contain equivalent solvent levels, prepared from noncomplexing solvent/nonsolvent mixtures. Because the purpose of this paper is to present the structure of membranes with graded density skins, the data supporting the interpretation of accelerated gelation kinetics and rapid desolvation is presented elsewhere.[27,31,32] Alteration of the Lewis acid : base complex components and their respective ratios not only permits manipulation of both the density gradient in the active separating layer and the underlying transition areas in the skin but the porosity of the supporting matrix. The oxygen plasma ablation studies on FP/FA and PA : NMP spun polysulfone hollow fiber membranes show that the latter not only has a thinner, less dense separating layer than its congener but that the resistance of its substrate to gas transport is significantly less. The more familiar bilayer membrane, comprised of a porous substructure and a thin skin of more uniform density, is a special case of the trilayer class. A bilayer membrane results when the density gradient in the skin approaches zero.

A model was developed which defined the resistance of the hollow fiber membrane (R) as the sum of the resistances of the separating layer (R_1) and the substrate (R_2)[28]:

$$R = R_1 + R_2 \tag{4}$$

where

$$R_1 = l/P \text{ (membrane)}$$

and

$$R_2 = l/P \text{ (substrate)}$$

Furthermore, the percent resistance of the substrate is defined as

$$\% \text{ resistance} = \frac{R_2}{R} \times 100 \tag{5}$$

Using this approach and the data in Tables I–III, the percent resistances of the matrices to gas transport of the uncoated, isopentane-treated, and Sylgard-coated 37% total solids polysulfone hollow fiber membranes were calculated. These percent resistances are given in Table IV. As can be seen in

TABLE IV
Percent Resistances of Hollow Fiber Membrane Substrate as Function of Treatment

	% Resistance		
System	Untreated	Isopentane-treated	Coated
FP/FA	28.6	27.1	25.1
PA : NMP	14.3	6.3	6.2

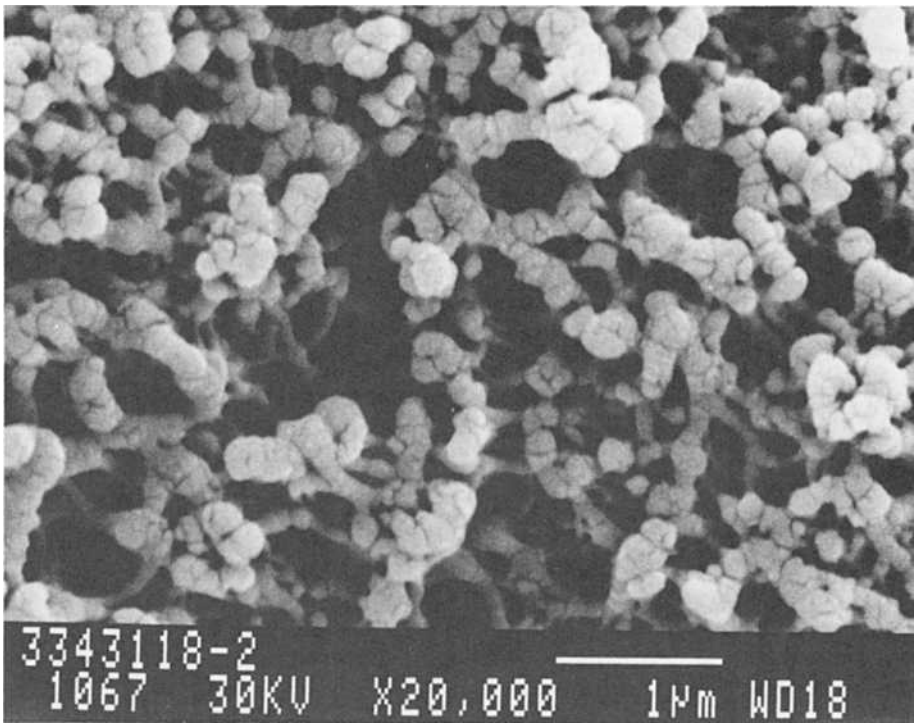

Fig. 10. Scanning electron micrograph of the substructure of an unetched, untreated hollow fiber membrane spun from PA : NMP complex.

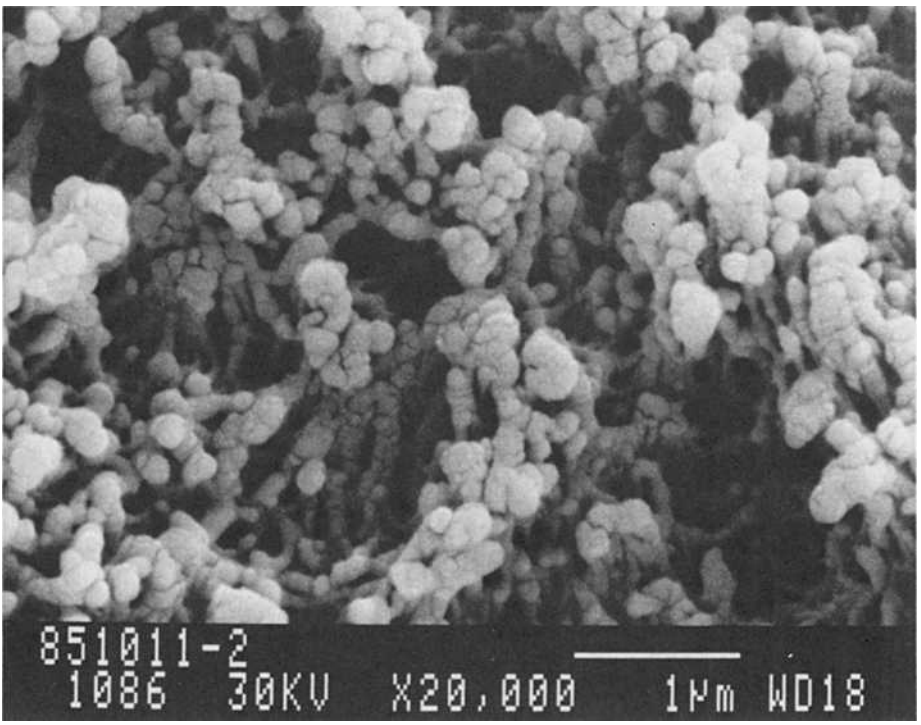

Fig. 11. Scanning electron micrograph of the substructure of an unetched, untreated hollow fiber membrane spun from FP/FA mixture.

Table IV, the matrix of the FP/FA spun hollow fiber membrane is a significant portion of the resistance to gas transport in even the coated membrane. This implies that the internal structure of this hollow fiber membrane is tighter and less open than the PA : NMP spun hollow fiber membrane. The latter hollow fiber membrane has much less internal resistance to flow, suggesting a much more open cellular structure with both higher porosity and lower tortuosity than that in the FP/FA spun hollow fiber membranes. These deductions based on the oxygen plasma ablation results were supported by scanning electron microscopy. Photomicrographs of the substructure of the PA : NMP spun hollow fiber membranes, as shown in Figure 10, reveal a more open structure with larger pore size than photomicrographs of the substructure of the hollow fiber membranes spun from FP/FA mixtures, as shown in Figure 11.

CONCLUSIONS

It is believed that membranes prepared from Lewis acid : base complex solvents possess a porous substructure and a nonuniform (graded density) skin which varies depending upon the gases to be separated, and a thin less dense transition layer, which may contain pores whose sizes are below the limits of resolution by SEM. Both are components of the microscopically observable skin. Membranes possessing this structure belong to the trilayer class of integrally skinned membranes. The more familiar bilayer integrally skinned separation membranes are a special case of the trilayer class in which the density gradient in the skin approaches zero to yield a membrane with a porous substructure and a thin skin of uniform density.

Oxygen plasma ablation is a viable technique to study the structure of hollow fiber membranes. Oxygen plasma ablation is amenable for membrane investigations because it is a low temperature process which does not thermally alter the membrane structure, and the plasma ablates only the membrane surface.

Oxygen plasma ablation studies on hollow fiber membranes spun from formylpiperidine/formamide and propionic acid : *N*-methylpyrrolidone dopes reveal differences in both the effective separating layers and internal matrix structures. The hollow fiber membranes spun from the FP/FA have active separating layer thicknesses, approximately 22.4 $\pm$ 2.2 nm, which are about twice that of the PA : NMP spun hollow fiber membranes. The active separating layer is not equivalent to the microscopically observable skin but is instead a fraction of it. Beneath the effective separating layer, there is a transition zone in which micropores, with sizes below the limit of resolution of the microscope, may reside. These proposed micropores increase in size and number as the region is traversed. Beneath this transitional zone is the porous supporting matrix itself. Oxygen plasma etching has shown that the hollow fiber membranes spun from PA : NMP complexes have thinner transition zones with a larger gradient of increase in pore size and porosity than do hollow fiber membranes spun from FP/FA. It was also shown that the coating carrier solvent alters the structure of both the effective separating layer and the porous substrate. Exposure to isopentane lowers slow gas transport rate and raises the selectivity of the hollow fiber membrane. This is attributed

primarily to a reduction in pores and defects in the active separating layer by isopentane abetted by a decline in the free volume in the active separating layer. Simultaneously, the transport rate through the porous matrix increases due to a reduction in the internal resistance attributed to increasing pore size and/or porosity of the matrix.

Finally, it was shown that the internal matrices of the hollow fiber membranes spun from PA : NMP have less resistance to flow than do those of hollow fiber membranes spun from FP/FA. This suggests that the former possess higher porosity, larger pore sizes, and lower tortuosities than the latter. As a result, the porous matrices of the PA : NMP complex spun hollow fiber membranes have lower resistance than those spun from FP/FA mixtures.

The authors wish to acknowledge the following individuals whose assistance was essential to the completion of the work reported herein: B. K. Daniels, M. H. Wade, C. J. Pellegrin, and M. H. Renth.

References

1. S. Loeb and S. Sourirajan, U.S. Pat. 3,133,132 (1964).
2. R. E. Kesting, *Synthetic Polymeric Membranes, A Structural Perspective*, 2nd ed., Wiley, New York, 1985.
3. J. M. S. Henis and M. K. Tripodi, U.S. Pat. 4,230,463 (1980).
4. R. H. Hansen, J. V. Pascale, T. Benedictus, and P. M. Rentzepis, *J. Polym. Sci. A*, **3**, 2205 (1965).
5. H. Yasuda, *Plasma Polymerization*, Academic, New York, 1985.
6. E. L. Lawton, *J. Appl. Polym. Sci.*, **18**, 1557 (1974).
7. R. H. Hansen, in *Interface Conversion*, P. Weiss and G. D. Cheevers, Eds., Elsevier, New York, 1969.
8. H. Yasuda, C. E. Lamaze, and K. Sakaoku, *J. Appl. Polym. Sci.*, **17**, 137 (1973).
9. G. A. Byrne and K. C. Brown, *J. Soc. Dyers Colour.*, **88**, 113 (1972).
10. M. Hudis, *J. Appl. Polym. Sci.*, **16**, 2397 (1972).
11. H. Schonhorn and R. H. Hansen, *J. Appl. Polym. Sci.*, **11**, 1461 (1967).
12. J. R. Hall, C. A. L. Westerdahl, A. T. Devine, and M. J. Bodnar, "Surface Treatment of Polymers with Activated Gas Plasma for Adhesive Bonding," Technical Report No. 3788, Picatinny Arsenal, Dover, NJ, January 1969.
13. J. R. Hall, C. A. L. Westerdahl, M. J. Bodnar, and D. W. Levi, *J. Appl. Polym. Sci.*, **16**, 1465 (1972).
14. H. Schonhorn, F. W. Ryan, and R. H. Hansen, *J. Adhesion*, **2**, 93 (1970).
15. N. J. DeLollis, *Rubber Chem. Technol.*, **46**, 549 (1973).
16. R. R. Sowell, N. J. DeLollis, H. J. Gregory, and O. Montoya, *J. Adhesion*, **4**, 15 (1972).
17. Y. Kitazaki and T. Hata, *J. Adhesion*, **4**, 123 (1972).
18. F. R. Anderson and V. F. Holland, *J. Appl. Phys.*, **31**, 1516 (1960).
19. F. R. Anderson, *J. Appl. Phys.*, **34**, 2371 (1963).
20. E. H. Harris and J. H. Magil, *Polymer*, **3**, 252 (1962).
21. M. R. Padhye, N. V. Bhat, and P. K. Mittal, *Text. Res. J.*, **46**, 502 (1976).
22. L. I. Bezruk and Y. S. Lipatov, International Symposium on Macromolecules, Leiden, The Netherlands, IUPAC, 1970, Vol. 2, p. 823.
23. A. K. Fritzsche, *Proc. Am. Chem. Soc. Div. Polym. Mater. Sci. Eng.*, **56**, 41 (1987).
24. R. E. Kesting, A. K. Fritzsche, M. K. Murphy, A. C. Handermann, C. A. Cruse, and R. F. Malon, U.S. and foreign patents applied for.
25. E. L. Lawton, *J. Polym. Sci. Polym. Chem. Ed.*, **10**, 1857 (1972).
26. E. L. Ringwald, *Polymer Handbook*, J. Brandrup and E. H. Immergut, Eds., Wiley-Interscience, New York, 1966.
27. A. K. Fritzsche, R. E. Kesting, and M. K. Murphy, *J. Membr. Sci.*, to appear.
28. J. M. S. Henis and M. K. Tripodi, *J. Membr. Sci.*, **8**, 233 (1981).

29. S. A. Stern, *Membrane Processes for Industry, Proceedings of the Symposium*, Southern Research Institute, 1966, p. 196.

30. S. T. Hwang, C. K. Choi, and K. Kammermeyer, *Sep. Sci.*, **9**, 461 (1974).

31. A. K. Fritzsche, M. K. Murphy, C. A. Cruse, R. F. Malon, and R. E. Kesting, in a paper presented at AIChE Symposium on Separation Science and Technology, Washington, DC, Nov.–Dec. 1988.

32. R. E. Kesting, A. K. Fritzsche, M. K. Murphy, C. A. Cruse, A. C. Handermann, R. F. Malon, and M. D. Moore, *J. Appl. Polym. Sci.*, to appear.

Received October 27, 1988
Accepted March 20, 1989